

Diffuse Scattering Models for mmWave V2X Communications in Urban Scenarios

Bogdan Antonescu

ECE Department

Northeastern University

Email: antonescu.b@husky.neu.edu

Miead Tehrani Moayyed

ECE Department

Northeastern University

Email: tehranimoayyed.m@husky.neu.edu

Stefano Basagni

ECE Department

Northeastern University

Email: basagni@ece.neu.edu

Abstract—This paper is concerned with the generation of accurate radio channel propagation models for mmWave transmissions for vehicle-to-everything (V2X) communications in urban scenarios. We emphasize the importance of capturing diffuse scattered rays for improved large-scale and small-scale radio channel propagation models. Our paper focuses on directive transmissions and compares various diffuse scattering models, arguing their advantage for the analysis of the mmWave radio links. The conclusions are that both received power levels and delay spread produce better estimates when the diffuse scatter models are enabled in the Wireless InSite ray-tracer that we use.

I. INTRODUCTION

Aiming at overcoming the many problems of current wireless networks, next generation (5G) wireless standards will provide unique features like ubiquitous connectivity, very low latency, and high-speed data transfers. One way to achieve these goals is through *spectrum extension* at frequencies in the *millimeter-wave* (mmWave) band (30–300 GHz) with its multiple GHz of unused bandwidth. Unlike sub-6 GHz wireless systems, communications in the mmWave spectrum suffer from higher propagation loss, sensitivity to blockage, atmospheric attenuation and diffraction loss. So, implementing transmissions at these high frequency bands brings in new challenges [1], [2]. These include range and directional transmissions, shadowing, fading due to atmospheric conditions, rapid channel fluctuations due to mobility, and multiuser coordination for increased spatial reuse and spectral efficiency.

In this paper we are concerned with providing an accurate radio channel propagation model for mmWave transmissions with *multipath fading*. For this study, we show that by considering various *diffuse scattering* models we improve the initial estimates of the root mean square (RMS) delay spread values and of the received power levels. Another contribution of our paper is the comparison between the use of isotropic vs. directive antennas for this analysis. While a higher gain can be obtained in isotropic transmissions when diffuse scattering is considered, we show that even for directive antennas, the extra gain in the received power is still relevant.

Our investigation uses Remcom's Wireless InSite [3] ray-tracer software tool, and focuses on the challenging

non line-of-sight (NLOS) transmissions that are an enabler for the communications in the mmWave spectrum. Through the proposed channel modeling and analysis we emphasize important design aspects of mmWave networks related to *directionality* of transmissions and the effect of various *beamwidths*.

The rest of the paper is organized as follows. Section II is a brief introduction to channel propagation modeling. Section III describes various models of diffuse scattering used in the literature in connection with multipath fading channel models. Section IV provides the results of our simulations for the scattering models and types of antennas that we use. Section V draws conclusions on the effects of diffuse scattering to channel propagation modeling in mmWave urban communications, and offers ideas for future research.

II. CHANNEL PROPAGATION MODELING

A suitable *radio channel model* is required to evaluate the performance of mmWave networks. It can be obtained through extensive measurements performed with steerable antennas and channel sounders, or via software ray-tracing simulators. In this paper we chose the latter option by using a professional tool (Wireless InSite) designed by Remcom. The advantage is the speed of producing viable results and the flexibility in making changes to the simulated scenario. Thus, as a first step, the ray-tracer provides a relatively quick methodology to estimate the challenges of designing a mmWave network for a specific use-case scenario.

In a radio channel, the received power is affected by attenuation characterized by a combination of three main effects: Path loss, shadowing loss and fading loss. The first two are important for characterizing the *large-scale* propagation model of the radio channel. The third one is mainly addressed in connection with the *small-scale* propagation model. This is the subject of our paper.

In a non-line of sight (NLOS) reception mode, the radio waves arrive at the receiver from different directions and with different propagation delays after reflection, diffraction and scattering. *Multipath components* (MPC) with randomly distributed amplitudes, phases and angles-of-arrival (AoAs) combine at the Rx causing the received

signal to distort or fade. Besides multipath, other factor that influences the small-scale propagation channel model is the *Doppler spread* due to mobility and speed of Tx and Rx (represented by cars, people and other moving objects). In a nutshell, the *small-scale effects* are considered rapid changes of the received signal strength over a small travel distance or time interval, random frequency modulation due to Doppler shifts, and time dispersion caused by multipath propagation delays.

Our analysis is concerned with *multipath fading* and provides a more comprehensive channel model that also includes diffuse scattering, besides the reflections and diffractions suffered by the traveling waves.

III. MULTIPATH AND DIFFUSE SCATTERING

One major concern in any wireless channel is *multipath*, which corrupts the wanted signal by producing distortions and time-delayed copies of the transmitted signal. To evaluate the channel time dispersive properties, we analyzed the *RMS delay spread* of the rays received at the receiver. The RMS (root mean square) value is similar to the standard deviation of a statistical distribution, and provides an indication about the severity of *Inter Symbol Interference* (ISI), which translates to more complicated schemes for symbol recovery at the receiver and in limitations of the maximum achievable channel data rate. As a rule of thumb, an RMS delay spread ten times smaller than the transmitted symbol time period guarantees no requirement for an ISI equalizer at the receiver.

Besides reflections and diffractions that are predominantly studied through measurements and simulations and thus captured in channel models, there is also scattering, which is much less considered and many times omitted. Thus, this section provides a brief overview of the *diffuse scattering* (DS) models considered in research literature. While scattering is not a new propagation model because it has been studied for sub-6 GHz frequencies, we can say that there are not many papers describing its effect in the mmWave spectrum. Our paper has the intention to fill-in this gap by producing more data for this topic while using a ray-tracer as a preliminary analysis tool.

Diffuse scattering refers to signals that are scattered in many directions, including the usual specular direction. These signals are generated because of gaps and sharp changes in the walls of a building that destroy its flat layer (e.g., windows, balconies, brick or stone decorations, beams). Last but not least, the type of material matters, creating an effective roughness parameter [4] for each wall that can be used with ray-based propagation tools.

The concept of diffuse scattering has been studied for many years. Starting with [5], continuing with microcellular propagation studies [6], and considering more recent works for both indoor [7], [8], [9] and

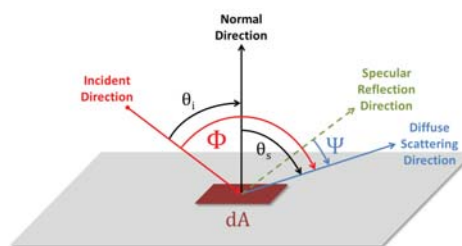


Fig. 1. Reflection and Diffuse Scattering from a surface [3].

outdoor [4], [10] mmWave transmissions, all have shown the importance of considering the effects of diffuse scattering. The conclusion is that multipath components resulted from diffuse scattering from building walls and other static or moving objects, in both indoor and outdoor scenarios, have to be considered in conjunction with channel characteristics (e.g., RMS delay spread, received power, angle of arrival) by comparing the effect of scattered fields with that of reflected/diffracted fields. Thus, various models for the DS propagation mechanism have been proposed. Three of the most well known DS models are the Lambertian model, the directive model and the directive with backscattering lobe model. Kirchhoff model is yet another model used for the general scattering geometry in which a wave is incident on a rough surface under angle θ with the normal to that surface, and is scattered to a direction given by elevation and azimuth angles. According to [11], this model provides good results if the surface does not contain sharp edges, spikes or other sharp irregularities, which is totally impossible to eliminate in many real use-case scenarios. Therefore, we will focus on the first three models mentioned above (Fig. 1).

In [6], the Lambertian model is applied, and the incident ray is partially reflected to the usual specular direction, partially transmitted and partially scattered with respect to the normal to the surface. The same model is used in [4] where an *effective roughness* is associated with each building wall by taking into consideration the real surface roughness as well as any wall discontinuities. Each wall has a scattering coefficient S and a reflection loss factor R that represents the loss of power in the specularly reflected wave.

In [10], a more realistic scenario is considered where the lobe of scattered rays is oriented toward the specular direction. This is the so-called *directive model*. It is stated that the shape of the scattering pattern strongly depends on the characteristics of wall irregularities. Therefore, three different kinds of scattering patterns are analyzed. The *Lambertian model* has its scattering radiation lobe in a direction perpendicular to the wall. The *Directive model* assumes a scattering lobe steered towards the specular reflection direction. Finally, the *Directive with Backscattering model* adds to the directive



Fig. 2. Urban V2X scenario: LOS and NLOS reception.

model an extra scattered lobe in the incident direction (i.e., backscattering phenomena); this effect can be experienced with protruding surface irregularities (e.g., balconies, columns). All three models can be used to predict the intensity of the scattered field, but careful consideration should be allocated to the polarization characteristics. Also, depending on the characteristics of the investigated use-case scenario, one model or the other could provide better results. In [10], the authors concluded that indeed the *directive model* performed best in all their simulations.

Other examples of papers that use the directive model include [8] for estimating the received power, RMS delay spread and maximum excess delay for an indoor scenario at 60 GHz, [12] for a more accurate channel characterization and estimation of the power delay profile (PDP) for 60 GHz indoor applications, and [7] where PDP, delay and angle characteristics models were better estimated by including diffuse scattering effects. In [9], both Lambertian and directive models were compared and used to estimate the PDP of indoor transmissions at 60 GHz, and included even a double bounce diffuse scattered wave for the Lambertian model following the description in [13].

IV. SIMULATION RESULTS

This section provides the results of our simulations, and emphasizes the role of capturing diffuse multipath components and of selecting the appropriate diffuse scattering model parameters, to provide a more comprehensive small-scale propagation channel model.

As mentioned in Section III, RMS delay spread is one important parameter that reflects the quality of the radio channel. To realize how RMS delay spread is affected by various transmission factors, we performed a series of experiments. We analyzed the effect of *beamforming* and *directional transmissions* as two very important techniques used in mmWave communications to combat path loss.

We simulated 28 GHz transmissions between transmitter and receiver units using one of the urban scenarios (Rosslyn, VA) delivered with the ray-tracing tool. The

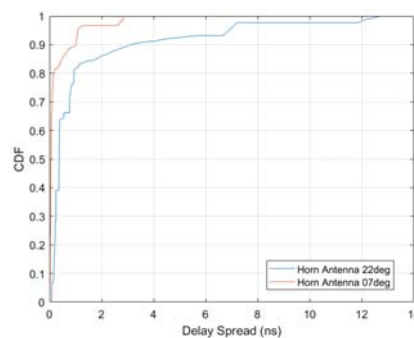
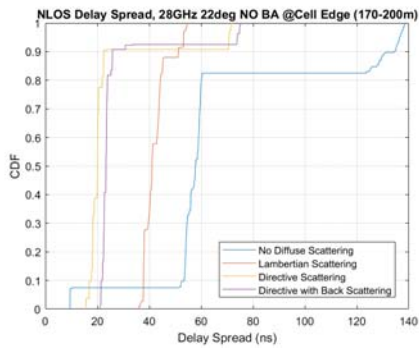
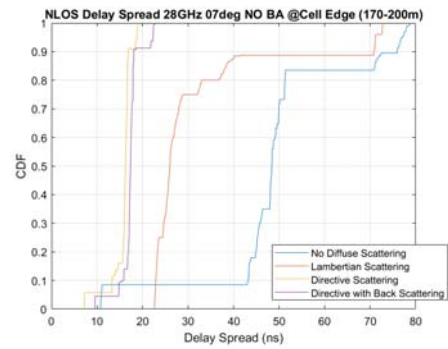


Fig. 3. Beamwidth effect in NLOS: Beam alignment.

Tx (base station) was located at a fixed site on a light/traffic pole (with a height of 8 m) in the North part of Fig. 2, and the Rx point was installed in a vehicle at approximately 1.5 m above ground. The LOS transmission was simulated in the North-South direction by placing the vehicle along the wide-open boulevard at different locations up to 150 m in front of the transmitter. The NLOS reception mode was simulated in the East-West orientation in Fig. 2 by moving the vehicle at distances 70 to 150 m from Tx, on a side street behind very tall buildings. Through the GUI of the ray-tracer, we selected two horn antenna models with different half-power beamwidth (HPBW) and gain ($7^\circ/25$ dBi and $22^\circ/15$ dBi). In all simulations described in this paper, the same antennas were used at both Tx and Rx locations. The transmitted signal had a maximum power of 24 dBm and a bandwidth of 800 MHz. The ray-tracer was set to follow a certain number of reflections (6) and diffractions (1) for each path from transmitter to receiver.

To prove the contribution of *directivity*, we used the NLOS scenario. At each Tx-Rx separation distance, we used Matlab to generate 300 random points (i.e., Rx points) that were given to the ray-tracer for simulation. The result was a decrease of the RMS delay spread value when the antenna beamwidth changed from 22° to 7° (Fig. 3). The reduction in beamwidth implies an increase in gain (15 dBi vs. 25 dBi). We mention that the two simulations used a *beam alignment* procedure in which the Rx orients its antenna to the direction associated with the most powerful signal received at that specific location. By doing that, the Rx latched on the strongest received rays that dominated the delay spread, so the result was smaller values for the RMS delay spread for both antenna beamwidths comparing with the same test closer to the edge of the cell (i.e., Tx-Rx separation of max. 200 m).

To realize the importance of *diffuse scattering*, we repeated our experiment by enabling this propagation model in our ray-tracer. Most of the available ray-tracers only account for rays that undergo specular reflections or


 Fig. 4. Scattering effect on RMS delay: 22° , no beam alignment.

 Fig. 5. Scattering effect on RMS delay: 7° , no beam alignment.

diffractions, failing to describe diffuse scattering, which can have a significant impact in estimating accurately the channel dispersion. The latest version of the Wireless InSite ray-tracer offers the option of using three types of diffuse scattering models (Lambertian, directive, and directive with backscatter), to increase the multipath richness of the simulation. We analyzed all three models and focused mostly on the NLOS case. The following sets of experiments considered the NLOS reception mode *at the edge* of the small cell (i.e., Tx-Rx separation of 170, 180, 190, and 200 m). In one simulation, we used $22^\circ/15$ dBi horn antennas with *no beam alignment* between the Tx and Rx antennas, and 100 random Rx points for each Tx-Rx separation distance. First, we ran the simulation without scattering. Then, we set the ray-tracer to include the effect of diffuse scattering for the three methods described above, and we ran three separate experiments. Plots of the cumulative distribution function (CDF) of the estimated *RMS delay spread* for these transmissions with and without scattering are presented in Fig. 4. The first observation is that RMS delay spread values are much bigger at the edge of the cell comparing with the ones shown in (Fig. 3) for locations closer to the transmitter. The directive and directive with backscatter models had the smallest RMS delay spread because they looked at the rays scattered in the same direction with the reflected rays, and thus all received rays arrived with small delays around the mean excess delay. Lambertian model looks at the rays scattered around the normal direction to the surface, so in that case the arrival times for any of those rays that might have been captured by the Rx antenna had a larger swing around the mean arrival time; hence, the slight increase in the RMS delay spread. The same positioning of the four plots is noticed in Fig. 5 for the $7^\circ/25$ dBi antennas, although (as expected) with smaller values of the RMS delay spread due to the increased gain and focus of the narrower beam antennas.

While all three scattering models used the same *no beam alignment* method (i.e., the Tx and Rx antennas

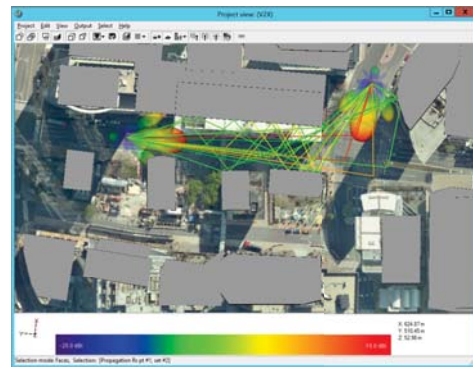
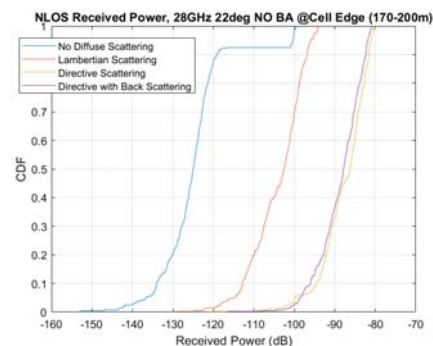
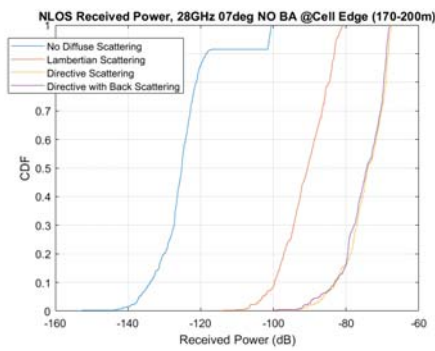
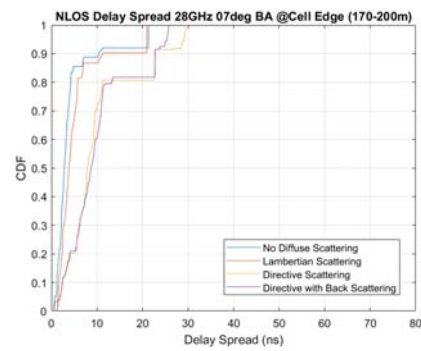
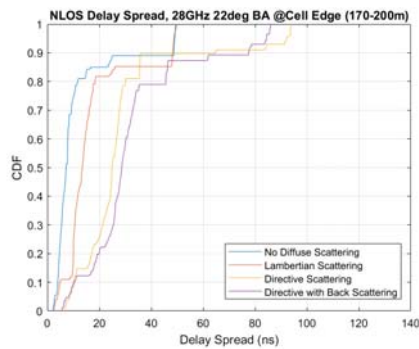
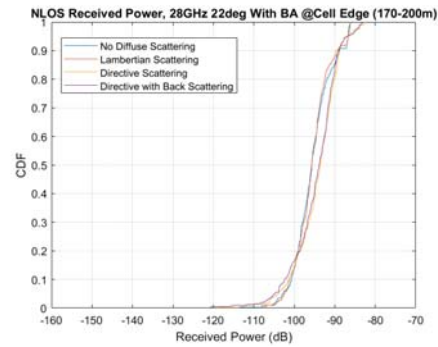


Fig. 6. No proper beam alignment of the Tx and Rx antennas.


 Fig. 7. Scattering effect on Rx power: 22° , no beam alignment.

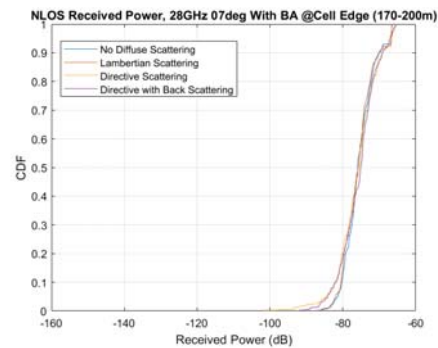
were simply oriented with the street direction Fig. 6), they still allowed the receiver to capture more rays comparing with case that didn't use any scattering. The improvement is even more visible if we analyze the *received power levels* for scattering vs. no scattering models. Fig. 7 (for $22^\circ/15$ dBi antennas) shows a substantial increase of the received power levels for the diffuse scattering models in comparison with the levels for the model that does not use any scattered rays. The reason for that is the reception of many more rays due to additional scattered lobes, not accounted initially. The larger increase in received power for the *directive model*


 Fig. 8. Scattering effect on Rx power: 7° , no beam alignment.

 Fig. 10. Scattering effect on RMS delay: 7° , beam alignment.

 Fig. 9. Scattering effect on RMS delay: 22° , beam alignment.

 Fig. 11. Scattering effect on Rx power: 22° , beam alignment.

proves that around the specular reflection direction there are many more scattered rays than around the normal to the surface. A similar increase in Rx power levels is noticed for the $7^\circ/25$ dBi antennas (Fig. 8).

To check the impact of *beam alignment*, we launched another set of simulations for which we recorded the RMS delay spread values as well as the received power levels. Fig. 9 shows the RMS delay spread for the $22^\circ/15$ dBi horn antennas, and proves that beam alignment is crucial for reliable mmWave communications. Without using any "help" from the scattered rays, the alignment of the two antennas allows the receiver to latch on the strongest rays that arrive close in time around the mean arrival time. The RMS delay value drops considerably for the classic reception that considers only reflections and diffractions. The RMS values for the receptions using scattering models remain in the same range as before, although we notice a much bigger influence of the beam alignment to the Lambertian scattering model than to the other two models. A similar model is followed by the $7^\circ/25$ dBi antennas (Fig. 10).

The fact that beam alignment is more important than an improvement of the channel propagation model that captures the effect of diffuse scattering is also confirmed by a barely noticeable difference in the values of the received power among the four studied models (Fig. 11).


 Fig. 12. Scattering effect on Rx power: 7° , beam alignment.

For the $22^\circ/15$ dBi horn antennas, the 2-3 dB difference in Fig. 11 vs. the large differences in received power in Fig. 7 shows that a more precise channel model that includes diffuse scattering always helps, but this improvement is minimal when beam alignment is used. The $7^\circ/25$ dBi horn antennas behave the same, but they show a bigger increase in Rx power levels and an even tighter differentiation among the four curves (Fig. 12).

The next set of experiments were concerned with the effect of Tx *antenna height* in NLOS reception. By placing the antenna on the side-wall of taller buildings or on top of them, it is possible to clear the height of

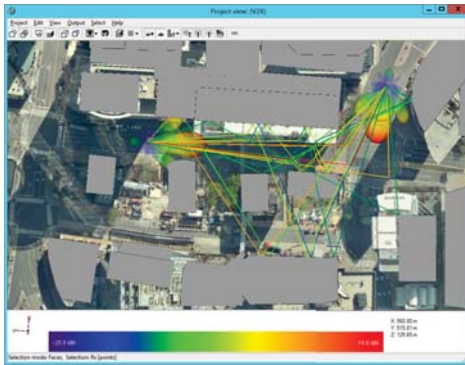


Fig. 13. Scattered rays for 30 m Tx height: 22°, no beam alignment.

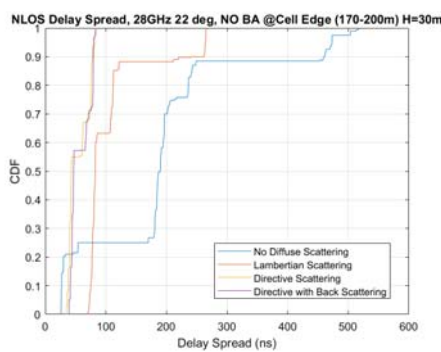


Fig. 14. RMS delay for 30 m Tx height: 22°, no beam alignment.

the smaller buildings that block the receiver. While this might represent an advantage because more reflections and diffractions might reach the receiver, all these much longer paths will lose power at each contact point with obstacles, which in the end will contribute to a bigger RMS delay spread. Using 22°/15 dBi horn antennas and having the transmitter elevated at 30 m, Fig. 13 shows many more rays arriving at the receiver in comparison with Fig. 6. Unfortunately, in this case, the "tunneling effect" of the reception on that side street is lost because the higher positioning of the Tx antenna creates many other much longer paths to the receiver. The RMS delay spread increases (Fig. 14), and the overall received power for the directive and directive with backscatter models is almost 10 dB smaller (Fig. 15), comparing with the case when the Tx height was 8 m (Fig. 4, Fig. 7).

In a final set of experiments, we changed the values of various parameters that influence the diffuse scattering transmission model. One of these parameters is the *scattering factor* (S) that shows the fraction of the incident electric field scattered diffusely, $S = |\vec{E}_S|/|\vec{E}_i|$. By doubling this parameter from 0.4 to 0.8 (i.e., capturing more diffuse scattered rays), we noticed a 5-10 dB increase in received power levels for all three diffuse scattering models (Fig. 16). The second parameter (α) models the shape of the forward lobe containing the diffuse scattered

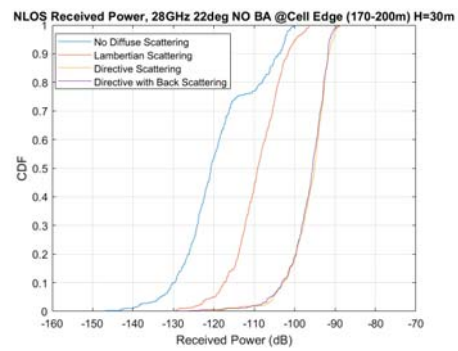


Fig. 15. Rx power for 30 m Tx height: 22°, no beam alignment.

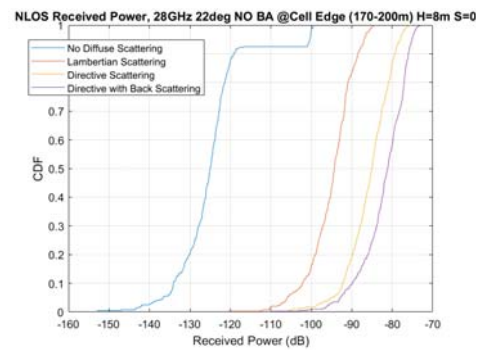


Fig. 16. Scattering factor effect on Rx power: 22°, no beam alignment.

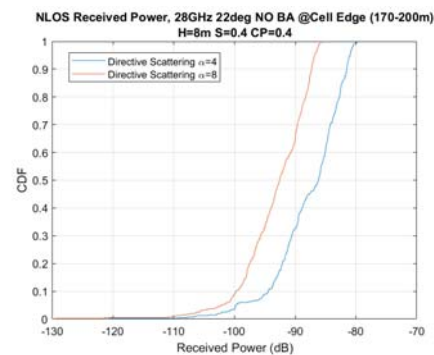


Fig. 17. Scattering forward-lobe size effect on Rx power.

rays centered on the direction of specular reflection. This parameter applies to both *directive* and *directive with backscatter* DS methods. The larger the value of α , the narrower the forward lobe is. Our simulations show that by doubling α (i.e., making the lobe narrower), we lose approximately 5 dB in the received power levels (Fig. 17). As last parameter, we increased the number of incident points that are captured in the diffuse scattering analysis, to check if our estimates with respect to received power improve or not. So far, we considered only the last obstacle that a ray hits before it reaches the receiver, and only for that point the three DS mechanisms

were applied. In this one last experiment, we allowed the ray-tracer engine to capture the effect of diffuse scattering at each obstacle hit by a ray from Tx to Rx. As expected, we took a big hit in simulation time (approx. 5.6 times longer). Unfortunately, all this effort showed almost no improvement comparing with the previous results. The only exception was an approx. 3 dB increase in the received power for the Lambertian model. Since the *directive* DS model is the most important mechanism, this model and the directive with backscattering are not influenced by considering extra analysis points on each ray trajectory. On the other hand, Lambertian model is not a dominant mechanism for DS, so any extra contribution from diffused scatter rays at each incidence point on the ray's path might bring at the receiver a little bit more power.

V. CONCLUSIONS AND FUTURE RESEARCH

As the standard for the next generation 5G wireless networks is getting more and more defined, having very accurate channel models for transmissions in the mmWave spectrum becomes a priority. Thus, our paper offered a way to improve these channels models by emphasizing the importance of *diffuse scattering* (DS) as a very plausible propagation mechanism in this spectrum. Using Wireless InSite, a professional ray-tracer tool, we analyzed two major characteristics of the radio transmissions that affect both the large-scale and the small-scale channel models (i.e., the received power and the RMS delay spread). Our results showed the clear advantage of considering various DS models when the beam alignment was not performed (i.e., the boresight of the Rx antenna was not aligned with the direction of the best reception). With this beam alignment in place, the gain was not relevant.

Our study used *directive* horn antennas, and confirmed the results and also the expectations (with respect to received power levels) of previous work done in [14] where the authors used only *isotropic* antennas. The Rx power metric and the quick analysis via ray-tracer are very important for the deployment of wireless networks because they offer a comprehensive view of *network coverage* in a certain area without performing expensive and time consuming measurements in the field. The other metric (RMS delay spread) is also important at the receiver for the reasons explained in Section III.

As future research, we plan to capture the effect of diffuse scattering from *multiple transmitters* and at different street intersections, and to quantify the DS effect on the Doppler spread, in addition to vehicle speed. Last but not least, we plan to migrate towards MIMO antenna arrays, to allow a better estimation of the power angular profile and of the Doppler spread and Coherence time of the radio channel.

ACKNOWLEDGMENTS

This work is supported in part by MathWorks under Research Grant "Cross-layer Approach to 5G: Models and Protocols." Particularly, we would like to thank Mike McLernon, Darel Linebarger and Paul Costa of MathWorks for their continued support and guidance on this project.

REFERENCES

- [1] Y. Niu, Y. Li, D. Jin, L. Su, and A. V. Vasilakos, "A survey of millimeter wave communications (mmWave) for 5G: opportunities and challenges," *Wireless Networks*, vol. 21, no. 8, pp. 2657–2676, April 2015.
- [2] S. Rangan, T. S. Rappaport, and E. Erkip, "Millimeter-Wave Cellular Wireless Networks: Potentials and Challenges," *Proceedings of the IEEE*, vol. 102, no. 3, pp. 366–385, March 2014.
- [3] Remcom, *Wireless InSite Reference Manual*, version 3.1.0 ed., Remcom, 315 S. Allen St., Suite 416, State College, PA 16801, June 2017.
- [4] V. Degli-Esposti, "A Diffuse Scattering Model for Urban Propagation Prediction," *IEEE Transactions on Antennas and Propagation*, vol. 49, no. 7, pp. 1111–1113, July 2001.
- [5] P. Beckmann and A. Spizzichino, *The Scattering of Electromagnetic Waves from Rough Surfaces*. New York, NY, USA: Pergamon Press, 1963.
- [6] V. Degli-Esposti and H. L. Bertoni, "Evaluation of the role of diffuse scattering in urban microcellular propagation," in *Proceedings of IEEE 50th Vehicular Technology Conference (VTC Fall)*, Amsterdam, The Netherlands, September 19–22 1999, pp. 1392–1396.
- [7] J. Jarvelainen and K. Haneda, "Sixty gigahertz indoor radio wave propagation prediction method based on full scattering model," *Radio Science*, vol. 49, no. 4, pp. 293–305, April 2014.
- [8] M. T. Martinez-Ingles, D. P. Gaillot, J. Pascual-Garcia, J. M. Molina-Garcia-Pardo, M. Lienard, and J. V. Rodriguez, "Deterministic and Experimental Indoor mmW Channel Modeling," *IEEE Antennas and Wireless Propagation Letters*, vol. 13, pp. 1047–1050, 29 May 2014.
- [9] J. Pascual-Garcia, J. M. Molina-Garcia-Pardo, M. T. Martinez-Ingles, J. V. Rodriguez, and N. Saurin-Serrano, "On the Importance of Diffuse Scattering Model Parameterization in Indoor Wireless Channels at mm-Wave Frequencies," *IEEE Access*, vol. 4, pp. 688–701, 8 February 2016.
- [10] V. Degli-Esposti, V. F. Fuschini, E. M. Vitucci, and G. Falciasecca, "Measurement and Modelling of Scattering From Buildings," *IEEE Transactions on Antennas and Propagation*, vol. 55, no. 1, pp. 143–153, January 2007.
- [11] C. Jansen, S. Priebe, C. Moller, M. Jacob, H. Dierke, M. Koch, and T. Kurner, "Diffuse Scattering From Rough Surfaces in THz Communication Channels," *IEEE Transactions on Terahertz Science and Technology*, vol. 1, no. 2, pp. 462–472, November 2011.
- [12] J. Pascual-Garcia, M. T. Martinez-Ingles, J. M. Molina-Garcia-Pardo, J. V. Rodriguez, and L. J. Llacer, "Using tuned diffuse scattering parameters in ray tracing channel modeling," in *Proceedings of the 9th European Conference on Antennas and Propagation (EuCAP)*, Lisbon, Portugal, April 13–17 2015, pp. 1–4.
- [13] L. Tian, V. Degli-Esposti, E. M. Vitucci, X. Yin, F. Mani, and S. X. Lu, "Semi-deterministic modeling of diffuse scattering component based on propagation graph theory," in *Proceedings of IEEE 25th Annual International Symposium on Personal, Indoor, and Mobile Radio Communication (PIMRC)*, Washington, DC, USA, September 2–5 2014, pp. 155–160.
- [14] D. Solomitckii, Q. C. Li, T. Balercia, C. R. C. M. da Silva, S. Talwar, S. Andreev, and Y. Koucheryavy, "Characterizing the Impact of Diffuse Scattering in Urban Millimeter-Wave Deployments," *IEEE Wireless Communications Letters*, vol. 5, no. 4, pp. 432–435, August 2016.